COBEM 2023 27TH INTERNATIONAL CONGRESS OF MECHANICAL ENGENEERING

ABCM Brazilian Society of Mechanical Sciences and Engineering
27th ABCM International Congress of Mechanical Engineering
December 04-08, 2023, Florianópolis-SC, Brazil

COB-2023-0083
LARGE EDDY SIMULATION OF THE ATMOSPHERIC FLOW AROUND WIND TURBINES WITH THE USE OF AN IMMERSED BOUNDARY METHOD

Leandro José Lemes Stival
João Marcelo Vedovotto
Aldemir Ap. Cavalini Jr.
Federal University of Uberlandia, School of Mechanical Engineering, Av. João Naves de Ávila, 2121, Uberlândia, MG, 38408-196, Brazil.
stival@ufu.br, vedovotto@ufu.br, aacjunior@ufu.br.

Fernando Oliveira de Andrade
Federal Technology University of Parana, Civil Construction, - Rua Deputado Heitor Alencar Furtado, 5000 - Ecoville CEP 81280-340 - Curitiba - PR - Brasil
fandrade@utfpr.edu.br

Abstract. *The wind energy has gained visibility in terms of progress and potential, especially in Brazil. The country has reached 21.5 GW of installed capacity in 2022 and already occupies the sixth position in the global ranking of onshore wind energy production. Besides that, the country has an impressive potential for offshore wind energy that easily exceeds 700 GWs. In this context, scientific research involving wind energy has shown significant progress, particularly the development of computational fluid dynamics coupled with approaches that fully resolve the wind turbine. The present study aims to apply Large Eddy Simulation (LES) along with the Immersed Boundary Method (IB) to provide crucial spatial and temporal information of the flow around selected wind turbines by performing analyzes. The numerical framework used in the simulations performs LES under a Cartesian block-structured mesh that is dynamically refined via an adaptive mesh refinement (AMR) to increase accuracy and reduce computational costs.*

Keywords: *Wind turbine, wake effect, computational fluid dynamics, large eddy simulation, immersed boundary method.*

1. INTRODUCTION

Wind energy has gained visibility in the last decade in terms of progress and potential, especially in Brazil. The Brazilian wind energy market has already advanced significantly. The country has reached 21.5 GW of installed capacity in 2022, with a total of 795 wind farms, and more than 9,000 wind turbines, and occupies the sixth position in the global ranking of onshore. Besides that, the country has potential for offshore wind energy that easily exceeds 700 GWs (ABEEÓlica, 2022). The amount of energy generated in a wind farm depends not only on wind availability but also in the potential of the wind that is being supplied. Therefore, it is essential to study the efficiency of wind power generation by assessing the effects of certain wind related parameters and coefficients on the wind turbine. A careful assessment of wind resources is desirable for the development of an effective wind project.

2. Governing Equations

In the present study, the evolution of the flow aerodynamics is described by the mass and momentum conservation equations. In cartesian coordinates and using index notation, for $i, j = 1, 2, 3$, these equations are given by:

$$\frac{\partial \rho}{\partial t} + \frac{\partial \rho u_i}{\partial x_i} = 0, \tag{1}$$

$$\frac{\partial \rho u_i}{\partial t} + \frac{\partial \rho u_i u_j}{\partial x_j} = -\frac{\partial p}{\partial x_i} + \frac{\partial \tau_{ij}}{\partial x_j} + f_i, \tag{2}$$

where p is the pressure, ρ is the fluid density, u_i is the velocity vector component for the i direction, τ_{ij} is the viscous stress tensor and $f_i$source term associated with forces of fluid-structure interactions is the component i of a source term associated with forces of fluid-structure interactions.

Then assuming an incompressible flow, since it does not have any heat transference consideration in the air flow,

considering Mach number lower than 0.3. Snel (2003) and Sanderse (2009) confirm the incompressibility assumption for wind power application, mainly based on the lower velocities in the wake region to justify.

A complete solution for the system that includes equations 1 and 2 by direct numerical simulation is quite complex, considering the computational effort required to represent all temporal-spatial scales in a high Reynolds Number flow. In particular, the flow over a wind power plant contains small eddies from the boundary layer of the blades to large ones that comprise many wind turbines (Mehta *et al.*, 2014). As a choice to address this problem, LES allows the modelling of particular eddies to reduce the degrees of freedom, which means removing certain information and then solving explicitly the remaining structures of the flow.

The LES method consists of applying a spatial filter in the transport equations, which enables the selection of the large eddies of the flow to be calculated explicitly, whereas appropriate models calculate the tiny structures. It is important to note that the most critical eddies to be explicitly solved at a wind power plant are the ones that will help to know about wind farm aerodynamics. These eddies, or turbulent structures, correspond to those of the size of the wind turbine blade, which are responsible for most of the momentum transportation.

3. Numerical Methods

The partial differential equations require solution by means of numerical methods developed in computer programs. The computational code applied in this work was written in FORTRAN, C and C++. The MFSim is code developed at Fluid Mechanics Laboratory (MFLab), located in Federal University of Uberlandia (UFU), which is based on the finite volume method and solves three-dimensional flow using conservative forms of mass and momentum equations. The code applies applies a block-structured regular and cartesian adaptive mesh refinement that reduces the computational cost, which is based on the finite volume method and solves three-dimensional flow using conservative forms of mass and momentum equations.

The finite volume method (FVM) is employed in this study to numerically simulate the mass and momentum conservation equations (PATANKAR, 1980). In the FVM the solution domain is divided into a finite number of elementary control volumes, considering that each centroid of the control volumes is the computational node. The computational domain is then composed by a collection of these nodes, which are the frame for the domain discretization and are independent of the reference coordinate system.

4. NREL 5MW

The simulation scenario developed in this work was based in a real scale case of an offshore wind turbine that was designed by NREL, called NREL 5 MW, it is one of the most reported turbine containing geometry information (Jonkman *et al.*, 2009). The reference case presents data in terms of aerodynamics coefficients and parameters, but not contain measurements of the downstream wake. The simulations will comprehend a complete real scale turbine where the properties of mean and turbulent flows will be analyzed and discussed, Table 1 gives an overview about the dimensions and operating conditions of the NREL 5MW.

Table 1. Parameters of the NREL 5MW Wind Turbine

Parameter	Value
Number of rotor blades	3
Rotor Diameter	126 m
Rated Power	5.3 MW
Rated Wind Speed	11.4 m/s
Rated Rotational Speed	12.1 rpm
Blade Length	61.5 m

For the MFSim simulations, the geometry of the NREL 5MW wind turbine was designed in the CATIA® software and meshed in the ICEM® CFD framework. Figure 1 illustrates the main components of the real scaled 5MW NREL wind turbine. With a rotor containing the 3 blades design, where the rotor diameter is equal to 126 m, characterizing the hub height at 90 m. The wind turbine mesh, which represents the lagrangian domain, contains a total of 67288 triangular cells. Where, 39465 cells represents the rotor geometry meanwhile 27823 cells characterizes the tower and nacelle as shown in Figure 1.

The inflow wind velocity profile was implemented at the inlet with a hub height velocity of u=8, v=0 and w=0 m/s, in the MFSim code, then characterizing a Dirichlet type of boundary condition. The boundary conditions for the lateral planes (xz-planes) were characterized as symmetry, this condition was also applied in the top plane (xy-plane). The

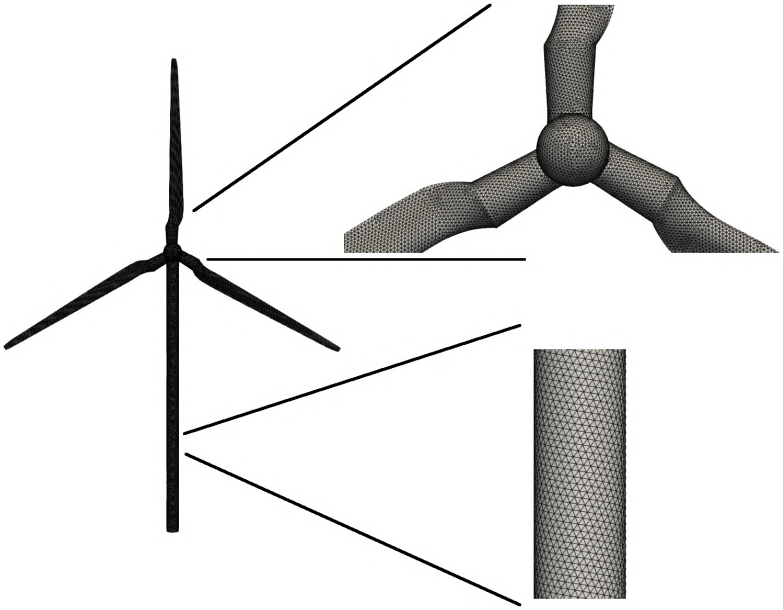

Figure 1. Lagrangian mesh of the NREL 5MW simulation

bottom plane (xy-plane) sets a no-slip condition in order to represent the ground where the turbine was placed in the wind tunnel. A Neumann boundary condition was used for pressure matters, meanwhile an advective condition was employed at the outflow condition, which is time varying to allow for vortical structures to cleanly exit the computational domain without reflecting back into the domain or disturbing the solution in the inner domain. The initial conditions of the simulations for velocities profiles at the hub height, u=8, v=0 and w=0 m/s. In these simulations, the fluid properties were ρ=1.225 kg/m³, μ=0.0000182 kg/(m s) and setting a Reynolds number ($Re \approx 2.46x10^6$) around the blade. It was adopted variable numerical time steps in the range of 10^{-4} to 10^{-5} s, maintained a CFL criteria of 0.5. The final simulation time was 1200 s. All statistics were calculated based on the last 500s of simulation or approximately 100 revolutions, period along which the flow presented approximately steady state conditions.

4.1 Geometry and Mesh Sensibility Analysis

This section presents quick analysis of how it was applied a sensibility analysis order to find the best geometry and mesh option to simulate the NREL5MW, done through sensitivity analysis with several simulations done until we got the best-fit option. Table 2 presents the simulations elaborated with the respective dimensions of the control volume in the directions x, y and z, with the levels of refinement applied as well as subdivisions for the cells of the coarsest level.

Table 2. Control Volume Cases for NREL 5MW Wind Turbine Simulation

	Control Volume Cases					
	A	B	C	D	E	F
X	1600 m	1600 m	1600 m	1600 m	1600 m	1600 m
Y	400 m	800 m	1000 m	1200 m	800 m	800 m
Z	300 m	500 m	500 m	500 m	800 m	600 m
Refinement Level	6	6	6	6	6	6
Subdivision	64 16 12	64 32 20	64 40 20	64 48 20	64 32 32	64 32 24

In terms of the control volume, the first attempt to simulate the NREL 5 MW considered the application of 300 m height with a 200 m width on each side (400 m) and a longitudinal distance of 1600 m. At the end of the simulation, a significant blockage influence occurred mainly in the z component related to the height of the domain. This simulation presented a blockage ratio value of 13.68%, as can be seen in Figure 2, which is a high value for simulation of this nature.

From the previous simulation result, an increase in the width and height of the simulation domain occurred. Therefore, for simulations B, C, and D, a height of 500 m in z was chosen, which would lead to less influence of the upper boundary condition of the domain on the flow while keeping the same longitudinal distance of 1600 m for direction x. Besides that,

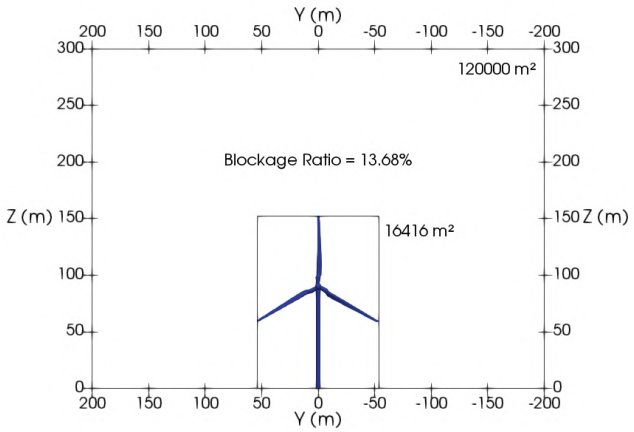

Figure 2. Case A

the widths in y were increased as well to values for (i) simulation B: 400 m on each side (800 m), (ii) simulation C: 500 m on each side (1000 m), and (iii) simulation D: with 600 m on each side (1200 m).

Simulation B, Figure 3, has a blockage ratio of 4.1%, while simulation C, Figure 4, shows a blockage ratio of 3.28%, while simulation D , Figure 5 reached a blockage ratio of 2.73%. All the simulations demonstrated a blockage ratio lesser than 5%, which is an acceptable value to simulate a case of this nature. The lateral influence of the walls was tiny and practically equal regardless of the simulation width, from 800 to 1200 m of the total width.

The height continued to have a small influence on the flow even with 500 m height. Such influence of the upper boundary condition had no effect in reflecting the flow back to the wake region. However, it might miss capturing some wake vortices that exceed 500 m height. For this reason, it was decided to create the simulation E, where the height in z increased to 800 m while the width value of 800 m in y was kept, since the width values presented similar results from 800 to 1200 m (simulation B to D), thus providing a lower computational cost for testing the flow at the chosen height.

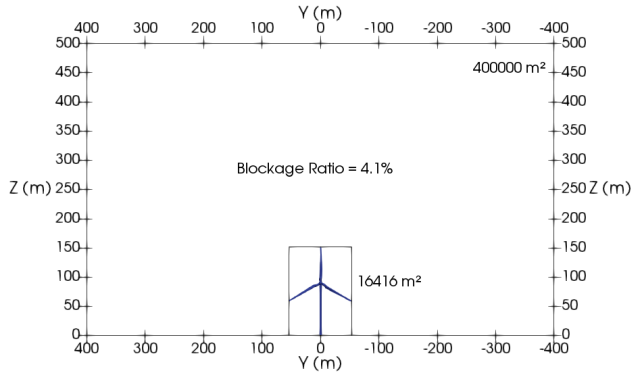

Figure 3. Case B

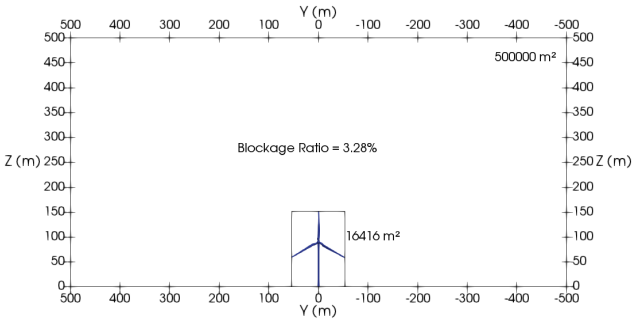

Figure 4. Case C

Simulation E, with values of x, y, and z of 1600, 800, and 800 m respectively, present a blockage ratio value of 2.65% considered very suitable for this type of simulation, as shown in Figure 6. It is possible to identify the influence of the

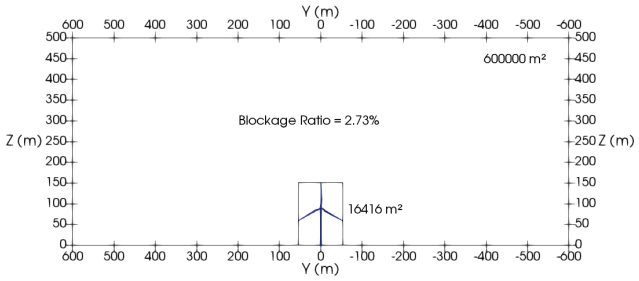

Figure 5. Case D

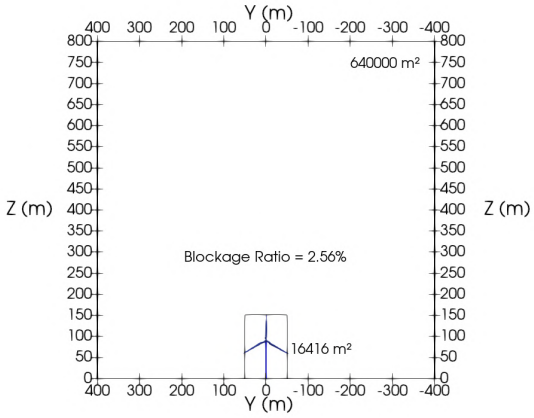

Figure 6. Case E

turbine on the downstream flow that occurs up to a height slightly above 500 m in z, indicating that a simulation with a height of 600 m in the direction z would be enough to capture all the influences of the wind turbine wake with a lower computational cost than when using 800 m of height.

Because of the eddies that still appear around 500 m height and the higher computational cost that lower blockage ratios would bring, a simulation with 800 m width and 600 m height was chosen for the final results. This setup presents a blockage ratio of 3.42 % that is within the standard applied to wind tunnel tests of less than 5-10% Choi and Kwon (1998). From this point on, all analyzes will consider 800 and 600 ratios for width and height.

Finally, four cases were performed to simulate the flow around the wind turbine, (i) applying the vorticity criteria and also by fixing a refinement region around the wind turbine and wake downstream with (ii) three, (iii) four, (iv) five levels of refinement, in order to understand how the behavior of the results would be with different approaches that are allowed in the MFSim code. Then, it was decided to use the most refinement case (five levels of refinement) to present

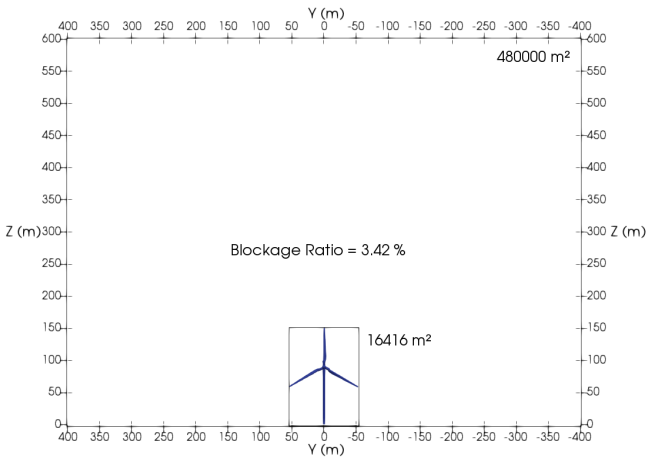

Figure 7. Case F - Final Setup

the following results in this scenario. The final simulation time was 1200 s, where the statistics were calculated based on the last 500s of simulation. The computational resource was based on two nodes of Intel Xeon E5650 2.67GHz 24-core machine utilizing approximately 26 GB RAM, the simulations required approximately 340 hours due its mesh with more than 3.5 millions of volumes.

4.2 Qualitative Analysis of the Flow Turbulent Structures

According to the definition, the Q-criterion defines vortices as areas where the vorticity magnitude is greater than the magnitude of the rate of strain. This section presents analyses to demonstrate that the LES-IB methodology is capable of simulating the interaction within the NREL 5 MW wind turbine and flow structures. Figure 8 shows a dynamic representation of the iso-surfaces colored by streamwise velocity, in order to provide important visualization of eddies occurring over the turbulent flow. Vortex structures occur in the region close to the blade's tip, which is transported over the flow forming helical shaped structures. These structures originate due to centrifugal flow acceleration, in which the fluid moves from the root towards the tip of the blade (Dasari *et al.*, 2019; Regodeseves and Morros, 2021). Therefore, the vortices structure patterns are straight connected to the turbine's operational parameters.

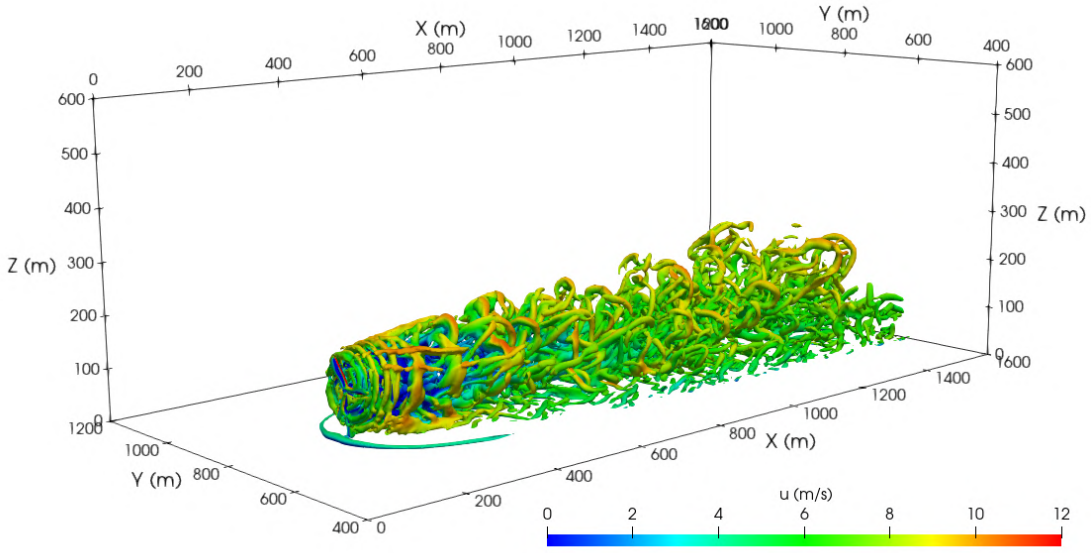

Figure 8. Dynamic iso-surfaces colored by velocity over flow around the wind turbine

Contours of the magnitude of the instantaneous gradients of velocity are plotted in Figure 9 to highlight the flow structures around the wind turbine. Figure 9(a) shows instantaneous velocity contours in an xy plane at the hub height, while Figure 9(b) displays the wind velocity on an xz plane at the centerline. It is possible to observe the development of different flow structures in the wake, depending on the distance and height analyzed, decreasing the intensity of the magnitude of the gradients transported to the far wake concerning the near wake while the size of the larger structures predominant in the far wake. The highest magnitude of the gradients above 4 (1/s) also occurs in the rotor region. Therefore, reaffirming the previous vorticity analysis that demonstrated high vorticity values were found over the same region.

As the most elevated vorticity and gradient intensities arose near the turbine, screenshots of instantaneous vorticity contours are shown to analyze this region of the turbine. Figure 10 shows the vorticity magnitude for the xz plane, at $x/D = 0$ around the turbine, where the highest vorticity values are densely scaled over the flow field. Therefore, it is possible to see that the highest vorticity densities occur mainly over the blade's area. More specifically, as shown in Figure 11, the vorticity values tend to increase from the blade's root to the blade's tip direction.

With that said, it was aimed to comprehend which gradient had the most contribution over this area. And following the mathematical definition of vorticity, as a curl of the velocity vector, $\bigtriangledown \times \vec{u} = \left(\frac{\partial w}{\partial x} - \frac{\partial v}{\partial z}\right)\vec{i} + \left(\frac{\partial u}{\partial z} - \frac{\partial w}{\partial x}\right)\vec{j} + \left(\frac{\partial v}{\partial x} - \frac{\partial u}{\partial y}\right)\vec{k}$. As the vector field is a velocity field in a flow, this measure indicates the rotation existing in the flow.

Figure 11 depicts the instantaneous gradient components contours around the swept area, where the most significant contributions come from the velocity gradients $\partial v/\partial x$ and $\partial w/\partial x$ concerning the spatial variation in the flow direction (x), primarily responsible for the downstream tip vortices structures Akay *et al.* (2014). Meanwhile, the sum of the contributions of $\partial w/\partial y$ and $\partial v/\partial z$, are accountable for the streamwise component of the vorticity, presenting the highest contribution on the leading edge of the blade's tip.

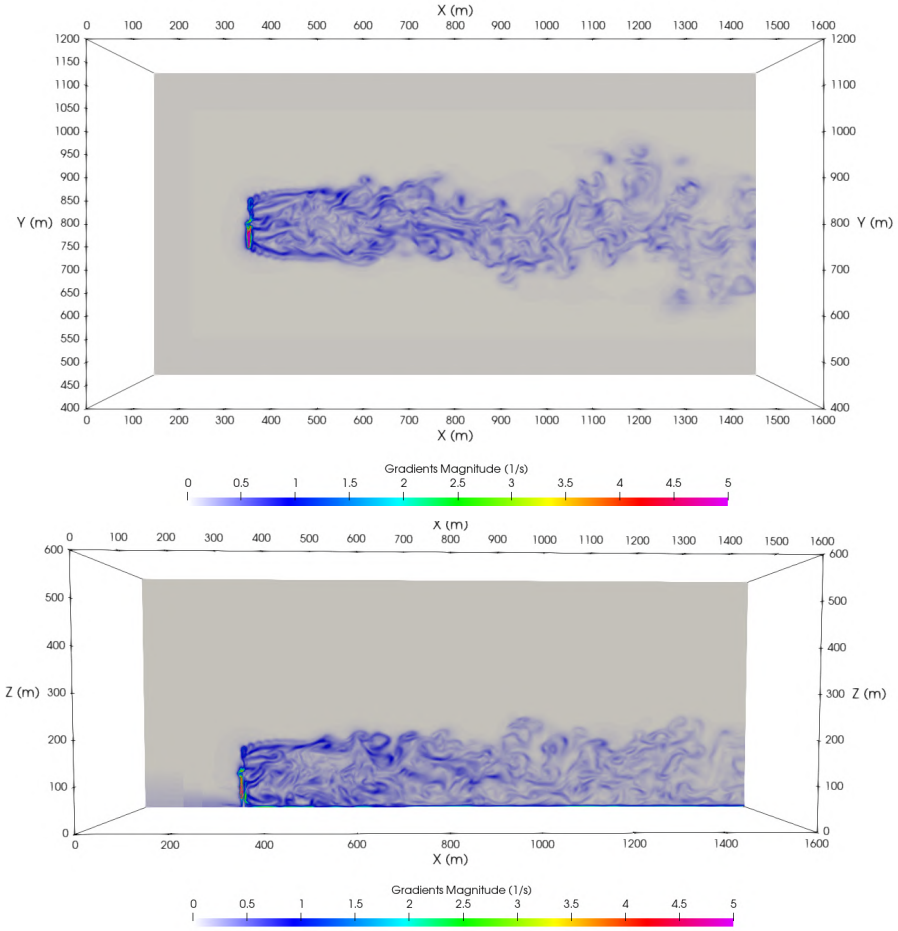

Figure 9. Contours of gradients over flow around the wind turbine, for (a) xy-plane, and (b) xz-plane

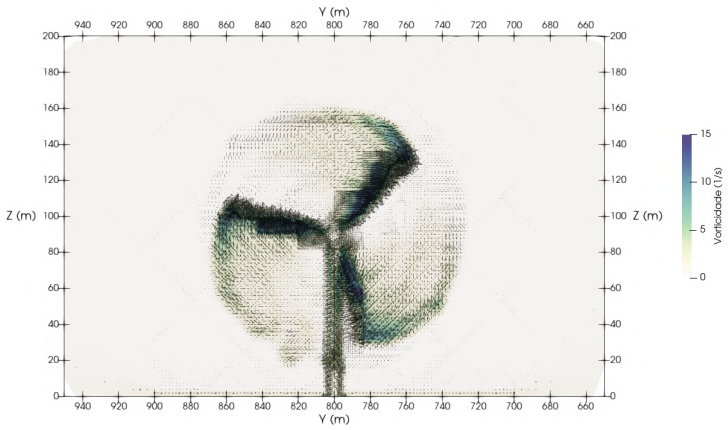

Figure 10. Vectors of vorticity magnitude in the downstream position of the wind turbine

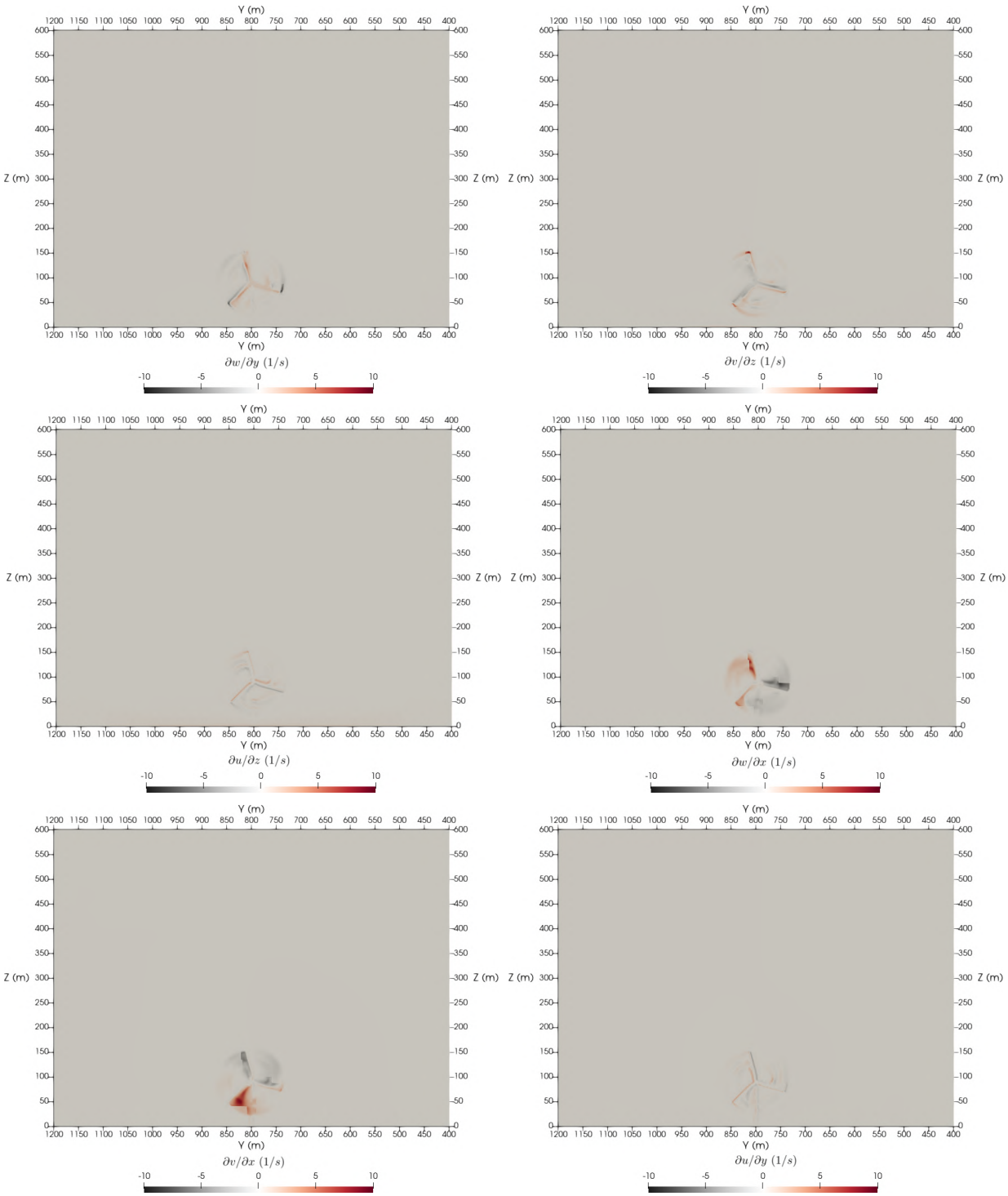

Figure 11. Contours of the gradient components around the swept area

4.3 Evaluation of Power Generation

Hence, in terms of torque, MFSim results presented a mean and standard deviation of 1873.89±73.90 (kNm), while the experimental study of the NREL 5MW Jonkman *et al.* (2009) showed a mean torque value of 1914.00 (kNm) for the same conditions, thus the mean difference corresponds to 40.11 (kNm), representing about a 2% difference between both results. In the case of power generation, mean values and standard deviation for the MFSim simulation corresponds to 1741.75±69.96 (kW). In contrast, NREL 5MW Jonkman *et al.* (2009) presented value of 1805.00 (kW), which results in a difference in generating power of 63.25 (kW). Therefore, a difference in power generation between both results is about 3.5%, which is a pretty low difference when take into consideration the size of the wind turbine that was applied in this work.

5. FINAL REMARKS

In conclusion of the third simulation scenario developed that it was based in a real scale case of an offshore wind turbine called NREL 5 MW. Firstly, it was decided to simulate the flow around the wind turbine with a control volume of 1600 m longitudinal, 800 m width, and 600 m height, reaching a blockage ratio around 3.42%. Then, simulations with five refinement levels over the wake was chosen in order to compare with the provided results. Regarding velocities evaluations, it was likely to distinguish high-velocity deficits in the near wake area immediately downstream from the wind turbine. Moreover, from qualitative analysis pointed out high velocities occurring around the blade tip around the swept area.

Lastly, the power production analysis demonstrated that low difference between the NREL report results and MFSim, leading to a lower than 3.5% difference for both torque and power generation, considering the turbine's size applied in the simulation.

6. ACKNOWLEDGEMENTS

The authors gratefully acknowledge the technical and financial support from Foz do Chapecó, Baesa, Enercan, and Ceran through the Research and Development project PD-02949-3007/2021 – "Solução integrada para o diagnóstico de defeitos, análise dinâmica e monitoramento contínuo de unidades gerado-ras francis" with resources from ANEEL's P&D program. The authors would also like to express their gratitude to CNPq, FAPEMIG, and CAPES (INCT-EIE) for the financial support of the present contribution.

7. REFERENCES

ABEEÓlica, 2022. "Abeeólica muda marca para oficializar atuação em eólica offshore e hidrogênio verde". *ABEEólica*. URL `https://abeeolica.org.br/`.

Akay, B., Ragni, D., Simão Ferreira, C. and van Bussel, G., 2014. "Experimental investigation of the root flow in a horizontal axis wind turbine". *Wind Energy*, Vol. 17, No. 7, pp. 1093–1109.

Choi, C.K. and Kwon, D.K., 1998. "Wind tunnel blockage effects on aerodynamic behavior of bluff body". *Wind and Structures An International Journal*, Vol. 1, pp. 351–364. doi:10.12989/was.1998.1.4.351.

Dasari, T., Wu, Y., Liu, Y. and Hong, J., 2019. "Near-wake behaviour of a utility-scale wind turbine". *Journal of Fluid Mechanics*, Vol. 859, p. 204–246. doi:10.1017/jfm.2018.779.

Jonkman, J., Butterfield, S., Musial, W. and Scott, G., 2009. "Definition of a 5-mw reference wind turbine for offshore system development". doi:10.2172/947422.

Mehta, D., van Zuijlen, A., Koren, B., Holierhoek, J. and Bijl, H., 2014. "Large eddy simulation of wind farm aerodynamics: A review". *Journal of Wind Engineering and Industrial Aerodynamics*, Vol. 133, pp. 1 – 17. ISSN 0167-6105. doi:https://doi.org/10.1016/j.jweia.2014.07.002. URL `http://www.sciencedirect.com/science/article/pii/S0167610514001391`.

PATANKAR, S.V., 1980. "Numerical heat transfer and fluid flow".

Regodeseves, P.G. and Morros, C.S., 2021. "Numerical study on the aerodynamics of an experimental wind turbine: Influence of nacelle and tower on the blades and near-wake". *Energy Conversion and Management*, Vol. 237, p. 114110. ISSN 0196-8904. doi:https://doi.org/10.1016/j.enconman.2021.114110. URL `https://www.sciencedirect.com/science/article/pii/S0196890421002867`.

Sanderse, B., 2009. "Aerodynamics of wind turbine wakes literature review".

Snel, H., 2003. "Review of aerodynamics for wind turbines". *Wind Energy*, Vol. 6, No. 3, pp. 203–211.

8. RESPONSIBILITY NOTICE

The authors are solely responsible for the printed material included in this paper.